

Adjustable Parameter Free Monte Carlo Simulation for Electron Transport in Silicon Including Full Band Structure

T. Kunikiyo, Y. Kamakura[†], M. Yamaji[†],
H. Mizuno[†], M. Takenaka[†], K. Taniguchi[†] and C. Hamaguchi[†]
LSI Laboratory, Mitsubishi Electric Corporation

[†] Department of Electronic Engineering, Osaka University, [‡] Sharp Corporation

1. Introduction

Electron transport in semiconductors has been investigated with use of Monte Carlo (MC) simulation by many authors[1][2][3]. In silicon, there are three major scattering mechanisms: scattering with ionized impurity, phonon scatterings and, at high electric field, impact ionization. The vast number of deformation potentials related to electron-phonon scattering are required to simulate transport throughout the entire Brillouin zone. Impact-ionization scattering is treated by using the Keldysh formula involving two adjustable parameters. Many authors have extracted deformation potential coefficients and these parameters in comparison between simulation and experimental results[2][3]. There still, however, exists large discrepancy in the values of these parameters. These fitting approaches, so called "parameter physics", fail to represent accurate feature of electron transport. The aim of this paper is to investigate the validity of an **adjustable parameter free** Monte Carlo simulator which employs electron-phonon scattering rates and impact-ionization scattering rate calculated with use of no adjustable parameters.

2. Calculation Procedure

The simulator includes the first five conduction bands calculated by using the empirical pseudopotential method[4], density of states and phonon dispersion relation calculated by using the adiabatic bond-charge model[5]. The simulator also employs electron-phonon scattering rates calculated by the rigid pseudo-ion model[6]. Wave functions of electrons given by the energy band calculation and polarization vectors of phonons given by phonon dispersion relation calculation are used for calculation of these scattering rates. Figure 1 shows total scattering rate calculated in the present work (solid line) and that obtained by using the non-parabolic band structure[2] (dashed line). The low-energy rates resemble closely the magnitude of the rates used in previous Monte Carlo work. Impact-ionization scattering rate, shown in Fig. 2, is calculated by using the Fermi golden rule directly including full band structure[7]. Wave vector dependent dielectric function is taken into account in the calculation of impact-ionization scattering rate. Impact-ionization scattering rate calculated in the present work strongly depends on both wave vector of electron and band index, shown by symbols in the figure. This is due to anisotropic nature of energy band structure of silicon. The simulator takes this point into account in calculation of impact-ionization coefficient. In MC calculation, final state of scattering electron is determined to conserve both energy and momentum in scattering processes.

3. Results and Discussion

Figure 3 shows calculated electron drift velocity along the $\langle 100 \rangle$ and $\langle 111 \rangle$ crystallographic directions as a function of time at various applied electric fields at 300K. At 100kV/cm, velocity overshoot along the $\langle 100 \rangle$ direction is larger than that along the $\langle 111 \rangle$ direction. This is due to

the difference of the effective masses near the X points in k-space. Figure 4 shows three snapshots of calculated electron distribution projected to cross-sectional plane normal to $\langle 001 \rangle$ axis in k-space at (a)0.05,(b)0.1,(c)0.15 picosecond after 100kV/cm electric field is applied along the $\langle 100 \rangle$ direction at 300K. At 0.05 picosecond, electrons near X points move to $\langle 100 \rangle$ direction keeping their elliptic distribution. This indicates that electrons are accelerated before they get enough energy. At 0.1 picosecond, the distribution slightly broadens due to electron-phonon scattering. At 0.15 picosecond, the distribution broadens more than before and the distribution around the $\langle 010 \rangle$ axis is no longer elliptic while the distribution around the $\langle 100 \rangle$ axis is still elliptic. This is due to the difference between longitudinal effective mass and transverse effective mass. Figure 5 shows calculated electron drift velocity along the $\langle 100 \rangle$ (solid line) and $\langle 111 \rangle$ (dashed line) directions as a function of applied electric field. Present results agree with experimental ones (symbols)[8] in all electric field regimes. Figure 6 shows calculated electron average energy (lines) as a function of applied electric field. Symbols denote calculated results by using non-parabolic energy band structure [8]. The present results are slightly smaller than conventional ones in high-electric field regimes. Figure 7 shows calculated electron diffusion coefficients (lines) as a function of applied electric field. Symbols denote experimental results along the $\langle 111 \rangle$ direction[1]. It appears that the discrepancy between longitudinal and transverse diffusion coefficients arises in high-electric field regimes. The agreement between the present results and experimental ones is very good in all electric field regimes. Figure 8 shows calculated impact-ionization coefficients (lines) and experimental results (symbols)[9][10] as a function of inverse of applied electric field. The present results agree with experimental ones[9][10].

4. Conclusions

We have investigated electron transport in silicon taking a full band structure, electron-phonon scattering rates and impact-ionization rates calculated with use of no adjustable parameters into account. We have evaluated electron drift velocity, average energy, diffusion coefficients, and impact-ionization coefficients at various applied fields. The present results agree with experimental ones, which confirms the validity of the newly developed MC simulator.

References

- [1] C.Jacoboni *et al.*, *Solid State Electron.*, **20**, p.77, (1977).
- [2] C.Jacoboni *et al.*, *Rev. of Mod. Phys.*, **55**, p.645, (1983).
- [3] M.V.Fischetti *et al.*, *Phys. Rev.*, **B 38**, p.9721, (1988).
- [4] M.L.Cohen *et al.*, *Phys. Rev.*, **144**, 789, (1966).
- [5] W.Weber *et al.*, *Phys. Rev.*, **B 15**, 4789, (1977).
- [6] P.B.Allen *et al.*, *Phys. Rev.*, **B 23**, p.1495, (1981).
- [7] N.Sano *et al.*, *Phys. Rev.*, **B 45**, p.4171, (1992).
- [8] C.Canali *et al.*, *Phys. Rev.*, **B 12**, p.2265, (1975).
- [9] Overstraeten *et al.*, *Solid State Electron.*, **13**, 583, (1970).
- [10] W.N.Grant *et al.*, *Solid State Electron.*, **16**, 1189, (1973).

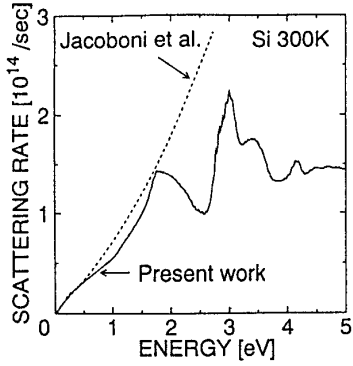


Figure 1 Phonon scattering rate.

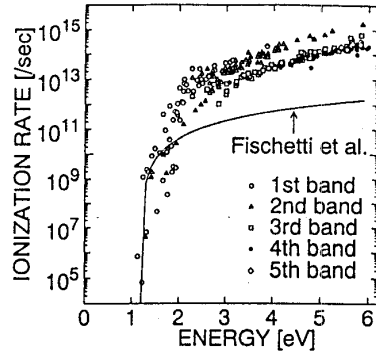


Figure 2 Impact-ionization rate.

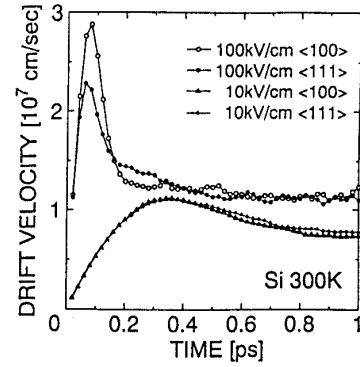


Figure 3 Calculated time dependence of electron drift velocity.

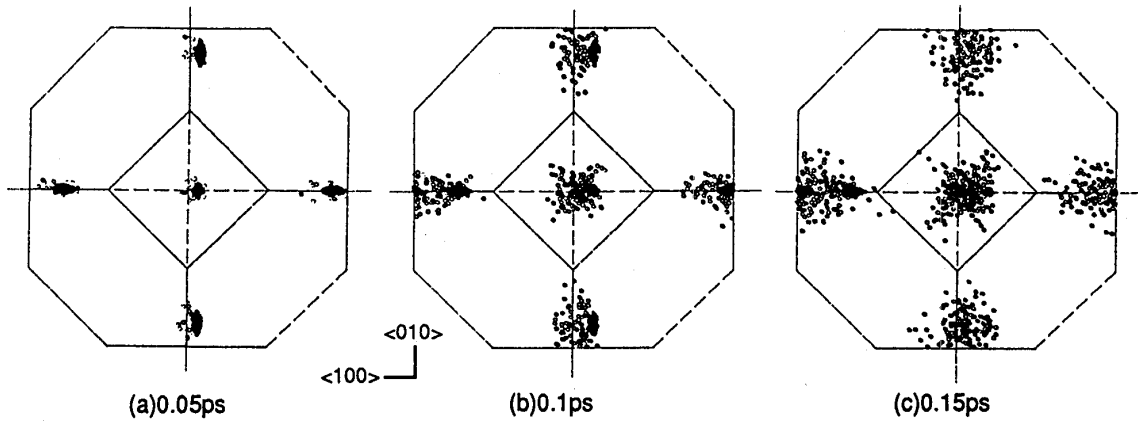


Figure 4 Snapshots of calculated electron distribution in k-space at (a)0.05,(b)0.1,(c)0.15 ps after 100kV/cm electric field is applied along the <100> crystallographic direction.

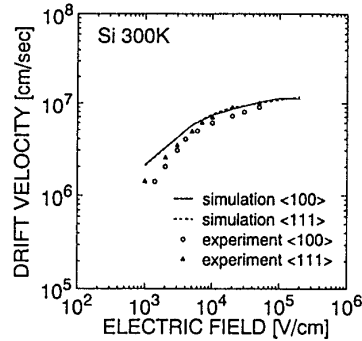


Figure 5 Drift velocity of electron as a function of applied electric field .

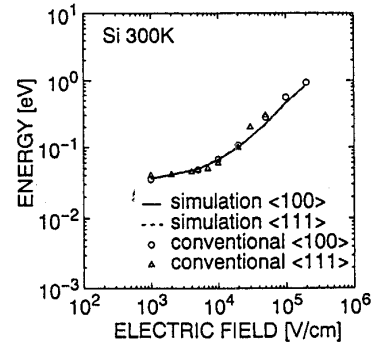


Figure 6 Calculated electron average energy .

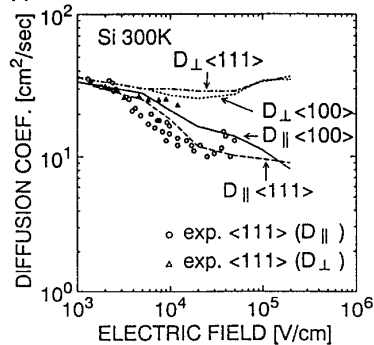


Figure 7 Diffusion coefficients of electron. D_{\parallel} , D_{\perp} denote longitudinal and transverse diffusion coefficient, respectively.

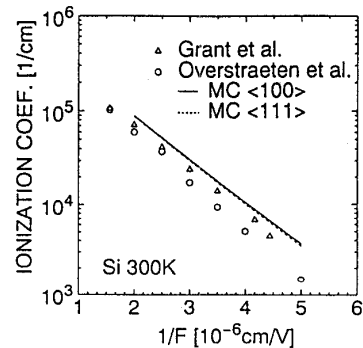


Figure 8 Impact-ionization coefficient.